# VII - Multirate Signal Processing and Filter Banks

There are many applications where the signal of a given sampling rate needs to be converted into an equivalent signal with a different sampling rate. Examples of such applications include digital audio and video. In order to achieve different sampling rates at different stages, multirate digital signal processing systems employ the down-sampler and the up-sampler, the two basic sampling rate alteration devices in addition to the conventional elements such as the adder, the multiplier and the delay. Discrete-time systems with unequal sampling rates at various parts of the system are called multirate systems.

Many multirate systems employ a bank of filters with either a common input or a summed output. These filter banks have efficient implementations that are attractive in the design of computationally efficient multirate systems. Filter banks are also important to separate signals into multiple channels, allowing the individual processing of certain

## A. Basic Sampling Rate Alteration

The two basic components in sampling rate alteration are the up-sampler and the down-sampler, which are introduced and analyzed in both time and frequency domains.

### Time-domain characterization:

An up-sampler with an up-sampling factor $L$, where $L$ is a positive integer, produces an output sequence $x_u[n]$ with a sampling rate that is $L$ times larger than that of the input sequence $x[n]$.

The up-sampling is implemented by inserting L-1 equidistant zero-valued samples between two consecutive samples of $x[n]$ according to

$$x_u[n] = \begin{cases} x[n/L], & n = 0, \pm L, \pm 2L, \ldots \\ 0, & \text{otherwise} \end{cases}$$

The up-sampler device has a block diagram representation shown in the figure below.

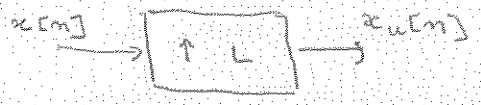


Fig.1 Block diagram representation of an up-sampler.

In practice, the zero-valued samples inserted by the up-sampler are replaced with appropriate nonzero values using some type of filtering process in order to ensure that the resulting higher-rate sequence is useful. This process is called interpolation.

The down-sampler with a down-sampling factor M, where M is a positive integer, develops an output sequence $y[n]$ with a sampling rate that is $(1/M)$th of the input sequence $x[n]$. The down-sampling operation is implemented by keeping every Mth sample of $x[n]$ and removing M-1 in-between samples to generate the output $y[n]$ as described by

$$y[n] = x[nM]$$

As a result, all input samples with indices equal to an integer multiple of M are retained at the output and all others are discarded.

A block representation of the down-sampler is shown in the figure below.

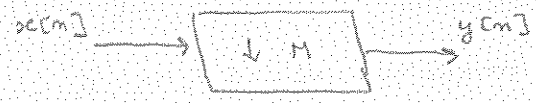


Fig. 2. Block representation of a down-sampler.

The operations of up-sampling and downsampling can be illustrated in the following figures.

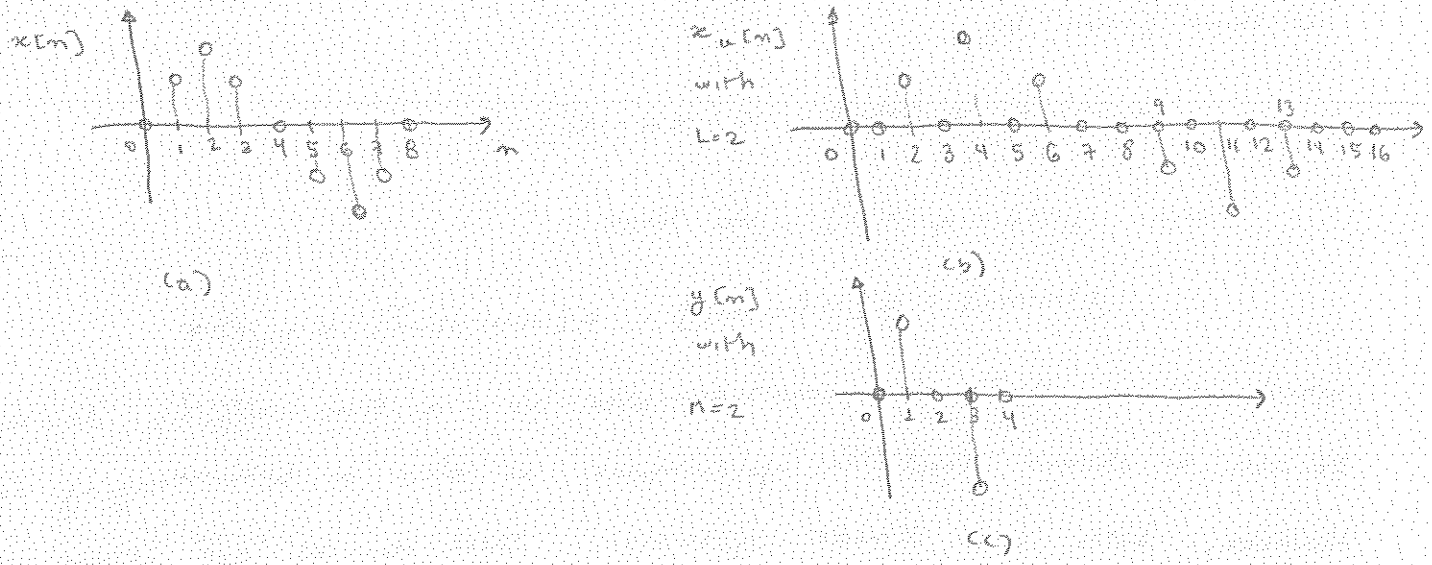


Fig 3 Illustration of b) up-sampling and c) downsampling operation on a) the original sequence.

In the exposition of multirate systems, we can also incorporate the sampling frequency $f_s = \frac{1}{T_s}$ into the signal alterations. The downsampling is described by

$$x[n] = x_a(nT_s) \longrightarrow \boxed{\downarrow M} \longrightarrow y[n] = x_a(nMT_s),$$

where the output sampling frequency is $f_s' = \frac{f_s}{M} = \frac{1}{MT_s}$.

The up-sampling is described by

$$x[n] = x_a(nT_s) \longrightarrow \boxed{\uparrow L} \longrightarrow x_u[n] = \begin{cases} x_a(nT_s/L), & n = 0, \pm L, \pm 2L, \ldots \\ 0, & \text{otherwise} \end{cases}$$

where the output sampling frequency is $f_s' = L \cdot f_s = \frac{L}{T_s}$.

The up-sampler and the down-sampler are linear but time-varying systems. The time-varying property of these devices is easy to show. Consider for example, the factor-of-M down-sampler $y[n] = x[nM]$. The output for an input $x_1[n] = x[n-n_0]$ is then given by

$$y_1[n] = x_1[Mn] = x[Mn - n_0].$$

From $y[n] = x[nM]$, we have

$$y[n-n_0] = x[M(n-n_0)] = x[Mn - Mn_0] \neq y_1[n],$$

which shows that the down-sampler is a time-varying device. It can be shown that the up-sampler is also a time-varying device. However, both are linear systems. These devices are often used together in application to change the sampling rate.

Frequency-domain characterization:

The relations between the spectra of the input and the output of an up-sampler with factor L can be derived as follows. Consider the output of the factor-of-L up-sampler:

$$x_u[n] = \begin{cases} x[n/L], & n = 0, \pm L, \pm 2L, \ldots \\ 0, & \text{otherwise} \end{cases}$$

In terms of the z-transform, the input output relation is given by

$$X_u[z] = \sum_{m=-\infty}^{\infty} x_u[m] z^{-m} = \sum_{\substack{m=-\infty \\ m \text{ even}}}^{\infty} x[m/L] z^{-m}$$

$$= \sum_{m=-\infty}^{\infty} x[m] z^{-Lm} = X[z^L].$$

The implication of the above relation on the unit circle can be illustrated by setting $z = e^{jw}$, which results in $X_u(e^{jw}) = X(e^{jwL})$. This can be illustrated by the DTFT $X(e^{jw})$ in the figure below.

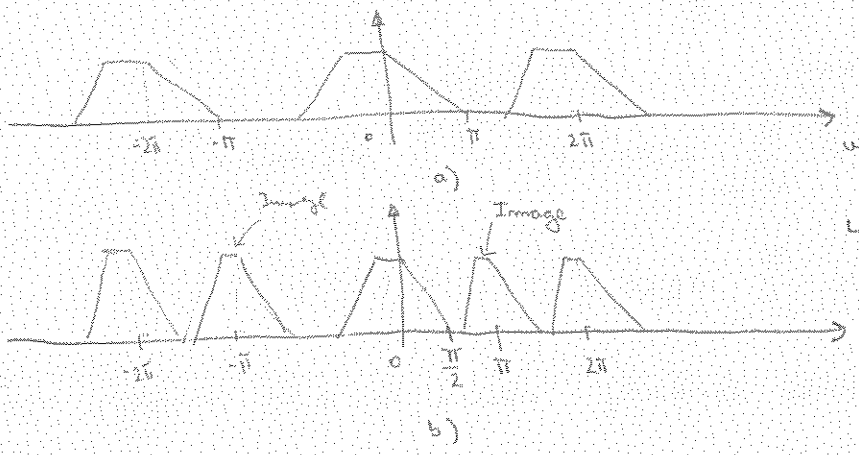


Fig. 4. Effects of upsampling in the frequency domain (a) Input sequence and (b) Output sequence for L=2

As shown in Fig. 4 a factor of L=2 leads to a 2-fold repetition of $X(e^{jw})$, indicating that the Fourier transform is compressed by a factor of 2. This process is called imaging because we get L-1 additional copies of the input spectrum in the baseband. Due to imaging the resulting spectrum after upsampling does not look like a low-frequency spectrum because of the insertion of zero-valued samples. Lowpass filtering of $x_u[n]$ removes the L-1 images or copies and fills in the zero-valued samples in $x_u[n]$ with interpolated values.

We now derive the relations between the spectra of the input and the output of a down-sampler. Applying the z-transform to the input-output relation $y[n] = x[nM]$, we arrive at

$$Y[z] = \sum_{n=-\infty}^{\infty} x[Mn]\, z^{-n}$$

The expression on the right-hand side of the above equation cannot be directly expressed in terms of $X[z]$. To solve this problem, we define an auxiliary sequence as given by

$$v[n] = \begin{cases} x[n] & , \quad n = 0, \pm M, \pm 2M \\ 0 & , \quad \text{otherwise} \end{cases}$$

Then, we have

$$Y[z] = \sum_{n=-\infty}^{\infty} x[Mn]\, z^{-n} = \sum_{n=-\infty}^{\infty} v[Mn]\, z^{-n}$$

$$= \sum_{k=-\infty}^{\infty} v[k]\, z^{-k/M} = V[z^{1/M}]$$

Now $v[n]$ can be formally related to $x[n]$ through $v[n] = c[n]\, x[n]$, where $c[n]$ is defined by

$$c[n] = \begin{cases} 1 & , \quad n = 0, \pm M, \pm 2M, \ldots \\ 0 & , \quad \text{otherwise} \end{cases}$$

A convenient representation of $c[n]$ is given by

$$c[n] = \frac{1}{M} \sum_{k=0}^{M-1} W_M^{kn},$$

where $W_M = e^{-j2\pi/M}$. Substituting $v[n] = c[n]\, x[n]$ and using the above value of $c[n]$ results in

$$Y[z] = \frac{1}{M} \sum_{k=0}^{M-1} X(z^{1/M} W_M^{-k})$$

To understand the implication of the above relation, consider a factor-of-$L=2$ down-sampler with an input $x[n]$ whose spectrum is shown in the next figure.

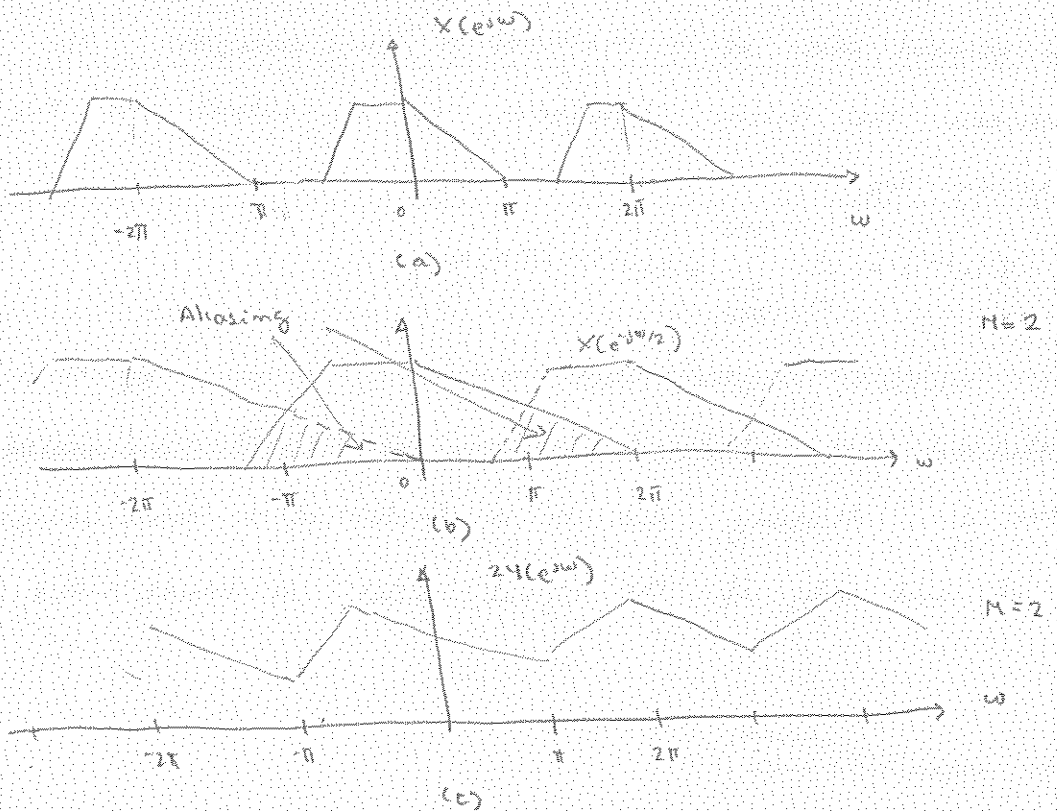


Fig. 5 Illustration of the aliasing effect in the frequency-domain caused by down-sampling

If we assume that $X(e^{jw})$ is a real function with an asymmetric frequency response, from $Y(z) = \frac{1}{M}\sum_{k=0}^{M-1} X(z^{1/M} W_M^{-k})$ we obtain

$$Y(e^{jw}) = \frac{1}{2}\left\{ X(e^{jw/2}) + X(e^{j(w/2)}) \right\}$$

To determine the relation of the 2nd term above with respect to the first, we observe that

$$X(e^{j(w/2)}) = X(e^{j(w-2\pi)/2}),$$

where $\frac{1}{2} X(e^{jw/2})$ is obtained by shifting the first term $X(e^{jw/2})$ to the right by $2\pi$, as shown in Fig 5 (b). The plots of the two terms $X(e^{jw/2})$ and $X(e^{j(w/2)})$ have an overlap, and the original shape of $X(e^{jw})$ is lost when $x[n]$ is downsampled. This overlap causes the aliasing. There is no overlap, i.e., no aliasing, only if $X(e^{jw})$ is zero for $|w| > \pi/2$.

For the general case of a factor-of-M down-sampler, the relations between the Fourier transform of the output and the input is given by

$$Y(e^{j\omega}) = \frac{1}{M} \sum_{k=0}^{M-1} X(e^{j(\omega - 2\pi k)/M})$$

The above relation implies that $Y(e^{j\omega})$ is a sum of $M$ uniformly shifted and stretched versions of $X(e^{j\omega})$ then scaled by a factor $\frac{1}{M}$. Aliasing due to a factor-of-M down-sampling is absent if and only if the signal $x[n]$ is bandlimited to $\pm \pi/M$.

Cascade equivalences.

In many applications, the basic sampling rate alteration devices and the filter components appear in a cascade form. We examine specific connections, their cost and equivalences, which leaves input-output relations invariant. It may be of interest to establish if the following connection is interchangeable:


It can be shown that this interchange is possible if and only if M and L do not have a common factor.

Other equivalences include the use of filters and can be useful in the analysis and design of more complicated systems:

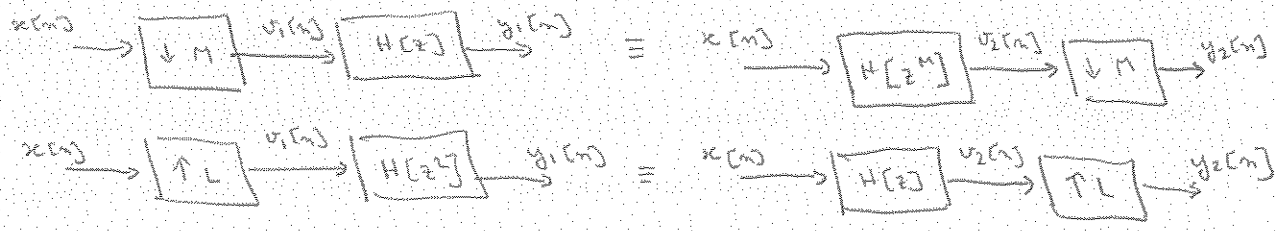

## B. Filters in Sampling Rate Alteration Systems

The bandwidth of a critically sampled signal must first be reduced by lowpass filtering before its sampling rate is reduced by a down-sampler. Likewise, the zero-valued samples introduced by an up-sampler must be interpolated to more appropriate values for an effective sampling rate increase. This interpolation can be achieved by digital lowpass filtering.

Filter specifications:

Since up-sampling causes periodic repetition of the basic spectrum, the unwanted images in the spectra of the up-sampled signal $x_u[n]$ must be removed by using a lowpass filter $H[z]$, called the interpolation filter, as indicated in Fig 6.


Fig. 6. Interpolation filter or interpolator.

On the other hand, prior to down-sampling, the signal $v[n]$ should be bandlimited to $|\omega| < \pi/M$ by means of a lowpass filter $H[z]$, called the decimation filter, to avoid aliasing caused by down-sampling. The system is shown in Fig. 7. below.

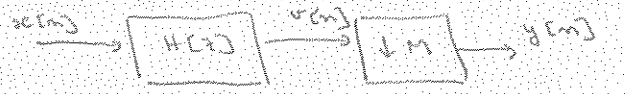


Fig. 7 Decimation filter or decimator.

In order to derive the specification for the lowpass filter, let us assume $x[n]$ has been obtained by sampling a bandlimited continuous-time signal $x_a(t)$ at the Nyquist rate. If $X_a(j\Omega)$ and $X(e^{j\omega})$ denote the Fourier transforms of $x_a(t)$ and $x[n]$, they are related through

$$X(e^{j\omega}) = \frac{1}{T_0} \sum_{k=-\infty}^{\infty} X_a\left(\frac{j\omega - j2\pi k}{T_s}\right),$$

where $T_s$ is the sampling period

Since the sampling is done at the Nyquist rate, there is no overlap between the shifted spectra of $X_a(j\omega T_s)$. If we instead sample $x_a(t)$ at a much higher rate $T = T_s/L$ resulting in $y[n]$, its fourier transform $Y(e^{j\omega})$ is related to $X_a(j\Omega)$ through

$$Y(e^{j\omega}) = \frac{1}{T}\sum_{k=-\infty}^{\infty} X_a\left(\frac{j\omega - j2\pi k}{T}\right)$$

$$= \frac{1}{T_s}\sum_{k=-\infty}^{\infty} X_a\left(\frac{j\omega - j2\pi k}{(T_s/L)}\right)$$

If we pass $x[n]$ through a factor-of-$L$ up-sampler generating $x_u[n]$, the relation between the fourier transforms $X_u(e^{j\omega})$ and $X(e^{j\omega})$ is given by

$$X_u(e^{j\omega}) = X(e^{j\omega L})$$

It follows from the above development that if $x_u[n]$ is passed through an ideal lowpass filter with a cutoff at $\pi/L$ and a gain of $L$, the output of the filter will be precisely $y[n]$.

In practice, a transition band is required to ensure the realizability and stability of the lowpass interpolation filter $H[z]$. Hence, the desired lowpass filter should have a stopband edge at $\omega_s = \pi/L$ and a passband edge $\omega_p$ close to $\omega_s$ to reduce the distortion of the spectrum of $x[n]$. If $\omega_c$ denotes the highest frequency that needs to be preserved in the signal to be interpolated the passband edge $\omega_p$ should be $\omega_p = \omega_c/L$. In summary, the specifications for the lowpass interpolation filter are

$$|H(e^{j\omega})| = \begin{cases} L, & |\omega| \le \omega_c/L, \\ 0, & \pi/L \le |\omega| \le \pi \end{cases}$$

Similarly, the specifications for the lowpass decimation filter are

$$|H(e^{j\omega})| = \begin{cases} A, & |\omega| \le \omega_c/M \\ 0, & \pi/M \le |\omega| < \pi, \end{cases}$$

where $\omega_c$ denotes the highest frequency that needs to be preserved in the decimation signal.

The effects of decimation and interpolation in the frequency domain are illustrated in the next figures for $M=2$ and $L=2$.

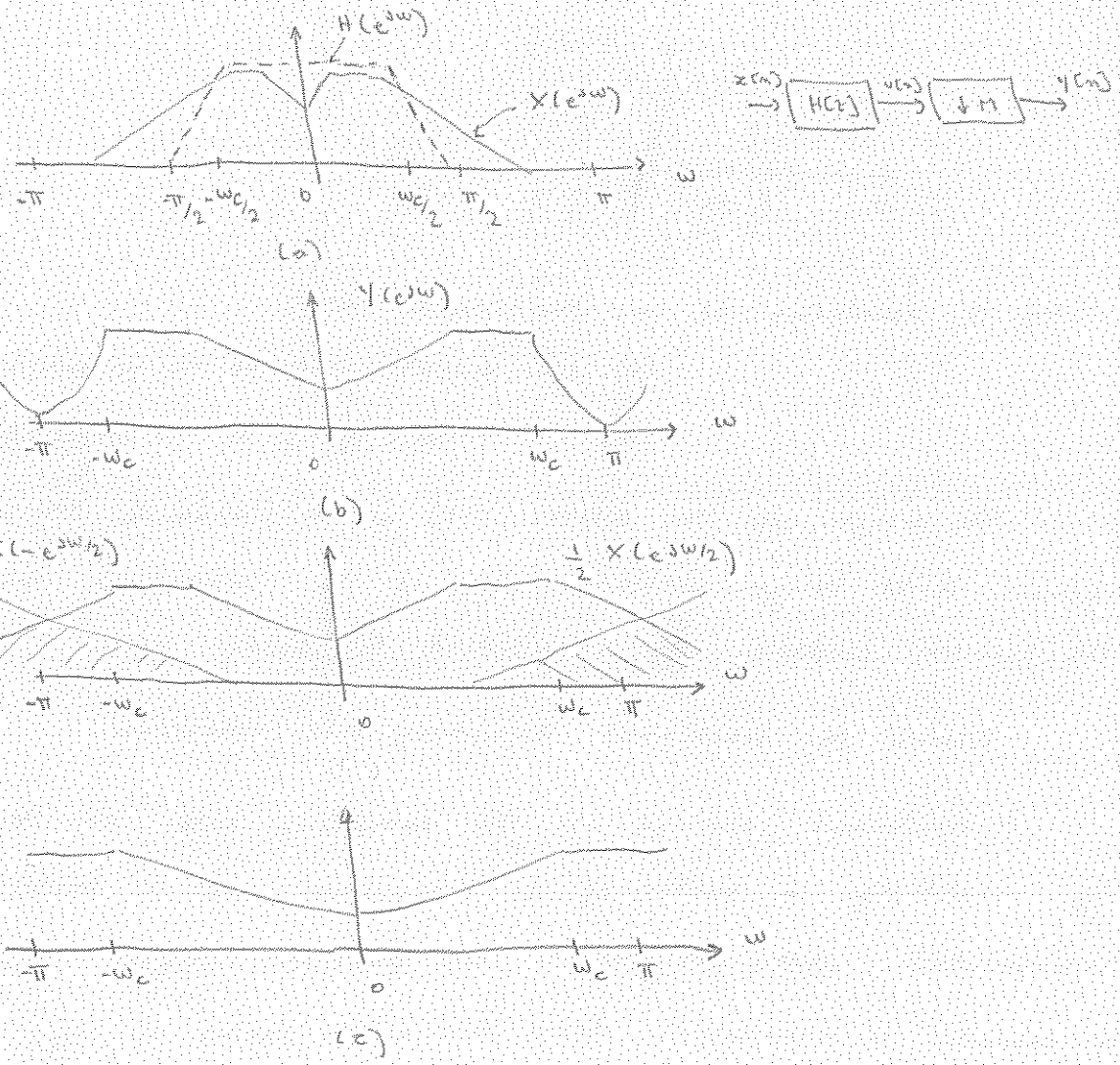





Fig 8. Spectrum of (a) the input $x(n)$
(b) the output $y(n)$ of the factor-of-2 decimator with $x(n)$ filtered
(c) the output $y(n)$ of the factor-of-2 decimator with no filtering of $x(n)$ showing the effect of aliasing

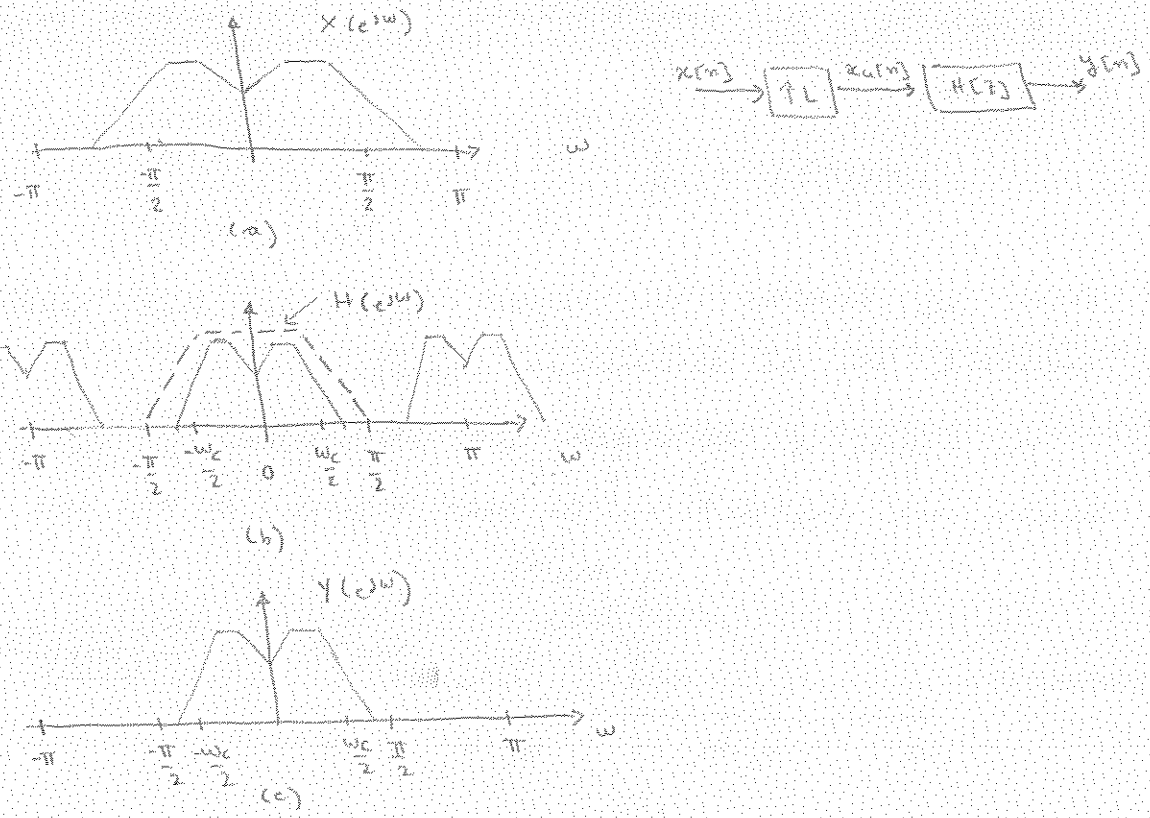


Fig. 9. Spectrum of (a) the input $x[n]$
(b) the output $x[n]$ of the up sampler
(c) the output $y[n]$ of the factor-of-2 interpolator

The design of the filter $H(z)$ is a standard IIR and FIR lowpass filter design problem. Any of the techniques discussed in the previous chapters can be applied to obtain $H(z)$.

## filters for fractional sampling rate alteration

A fractional change in the sampling rate can be achieved by cascading a factor-of-$M$ decimator with a factor-of-$L$ interpolator, where $M$ and $L$ are positive integers. Such a a cascade is equivalent to a decimator factor of $M/L$, or alternatively, to an interpolator with an interpolation factor of $L/M$. There are two possible cascade connections for sampling rate alteration as illustrated in the nuext figure.

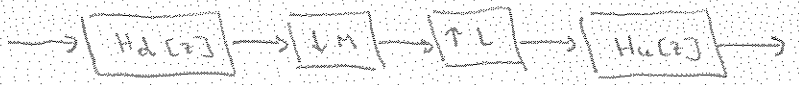


(a)


(b)

Fig. 10 General schemes for increasing the sampling rate by $L/M$.

The scheme in Fig. 10 (b) is more efficient since only one of the filters, $H_u[z]$ or $H_d[z]$, is adequate to serve as the interpolation filter and the decimation filter, depending on which one of the two stopband frequencies, $\pi/L$ or $\pi/M$, is a minimum. The preferred configuration for the fractional sampling rate alteration is as indicated in Fig 10 (c), where the lowpass filter $H[z]$ has a normalized stopband cutoff frequency at

$$\omega_s = \min\left(\frac{\pi}{L}, \frac{\pi}{M}\right),$$

which suppresses the imaging caused by the interpolator while at the same time ensuring the absence of aliasing that would otherwise be caused by the decimator.

Computational Requirements:

Consider the factor-of-$M$ decimator structure described by

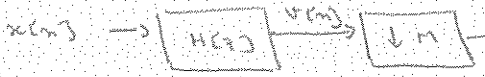


If the decimation filter $H[z]$ is an FIR filter of length $N$ implemented in a direct form, then

$$v[n] = \sum_{m=0}^{N-1} h[m] \cdot x[n-m]$$

Now, the downsampler keeps only every Mth sample of $v[n]$ at its output. As a result it is sufficient to compute $v[n]$ using the previous equation only for values of $n$ that are multiples of $M$ and skip the computations of the intermediate $M-1$ samples. This leads to a factor of $M$ saving in computational complexity.

If $H[z]$ is an IIR filter of order $K$ with a transfer function

$$H[z] = \frac{V[z]}{X[z]} = \frac{P[z]}{D[z]},$$

where $P[z] = \sum_{n=0}^{K} p_n z^{-n}$ and $D[z] = 1 + \sum_{n=1}^{K} d_n z^{-n}$.

Its direct implementation is given by

$$w[n] = -d_1 w[n-1] - d_2 w[n-2] - \ldots - d_K w[n-K] + x[n],$$

$$v[n] = p_0 w[n] + p_1 w[n-1] + \ldots + p_K w[n-K].$$

Since $v[n]$ is being down-sampled, it is sufficient to compute $v[n]$ using $v[n]$ only for values of $n$ that are integer multiples of $M$. However, the intermediate signal $w[n]$ above must be computed for all values of $n$. For example, in the computation of

$$v[M] = p_0 w[M] + p_1 w[M-1] + \ldots + p_K w[M-K],$$

$K+1$ successive values of $w[n]$ are still required. As a result, the savings in the computations in the case of an IIR filter is going to be less than a factor of $M$.

For the case of the interpolation filter similar arguments hold. If $H[z]$ is an FIR filter, then the computational saving is by a factor of $L$. On the other hand, the savings are less significant with IIR filters.

Matlab:

The main functions used for sampling rate alteration are

- decimate
- interp
- resample.

## C. The Polyphase decomposition

The polyphase decomposition can lead to computationally efficient realization of FIR filters. Moreover, it can also help in the efficient realization of the decimator and the interpolator.

Consider an arbitrary sequence $x[n]$ with a z-transform $X(z)$:

$$X(z) = \sum_{n=-\infty}^{\infty} x[n] \cdot z^{-n}$$

This z-transform can be rewritten as follows:

$$X(z) = \sum_{k=0}^{M-1} z^{-k} \sum_{m=-\infty}^{\infty} x_k[m]\, z^{-m}$$

$$= \sum_{k=0}^{M-1} z^{-k} \sum_{m=-\infty}^{\infty} x[Mm+k]\, z^{-m}, \quad 0 \le k \le M-1$$

$$= \sum_{k=0}^{M-1} z^{-k}\, X_k[z^M]$$

The subsequences $x_k[n]$ are called the polyphase components of the parent sequence $x[n]$ and the functions $X_k[z]$, given by the z-transform of $x_k[n]$, are called the polyphase components of $X[z]$. The relation between the subsequences $x_k[n]$ and the original sequence $x[n]$ is given by

$$x_k[n] = x[Mn+k], \quad 0 \le k \le M-1$$

The z-transform can also be written in matrix form as

$$X(z) = \begin{bmatrix} 1 & z^{-1} & \cdots & z^{-(M-1)} \end{bmatrix} \begin{bmatrix} X_0(z^M) \\ X_1(z^M) \\ \vdots \\ X_{M-1}(z^M) \end{bmatrix}$$

A multirate structural representation of the polyphase decomposition is shown below.

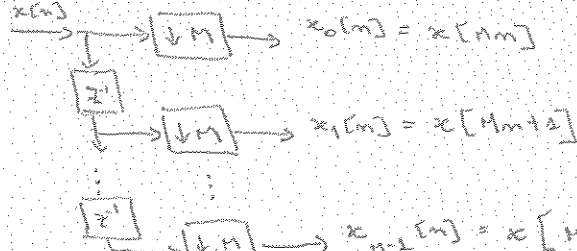


Fig. 11 An M-band polyphase decomposition of $x[n]$

The polyphase decomposition can be illustrated using an FIR transfer function $H[z]$ of length 6:

$$H[z] = \sum_{k=0}^{5} h[k]\, z^{-k} = h[0] + h[1]z^{-1} + h[2]z^{-2} + h[3]z^{-3} + h[4]z^{-4} + h[5]z^{-5}$$

Expressing the above as a sum of two terms, we obtain

$$H[z] = (h[0] + h[2]z^{-2} + h[4]z^{-4}) + (h[1]z^{-1} + h[3]z^{-3} + h[5]z^{-5})$$

$$= (h[0] + h[2]z^{-2} + h[4]z^{-4}) + z^{-1}(h[1] + h[3]z^{-2} + h[5]z^{-4})$$

Using the notation

$$E_0[z] = h[0] + h[2]z^{-2} + h[4]z^{-4}$$

$$E_1[z] = h[1] + h[3]z^{-2} + h[5]z^{-4},$$

we can rewrite $H[z]$ as

$$H[z] = E_0[z^2] + z^{-1}E_1[z^2],$$

which has a structural representation as shown in Fig. 12.

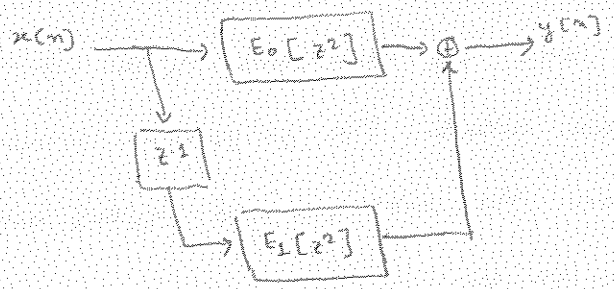


Fig. 12 Polyphase decomposition of an FIR transfer function.

In the general case, an M-branch polyphase decomposition of a transfer function $H[z]$ of order $N$ can be written as

$$H[z] = \sum_{k=0}^{L-1} z^{-k} E_k[z^M]$$

where $E_k[z] = \sum_{n=0}^{\lfloor (N+1)/M \rfloor} h[Mn + k]\, z^{-n}$, $0 \le m \le M-1$ and

$h[n] = 0$ for $n > N$.

A realization of the previously described polyphase decomposition is illustrated in Fig. 13.

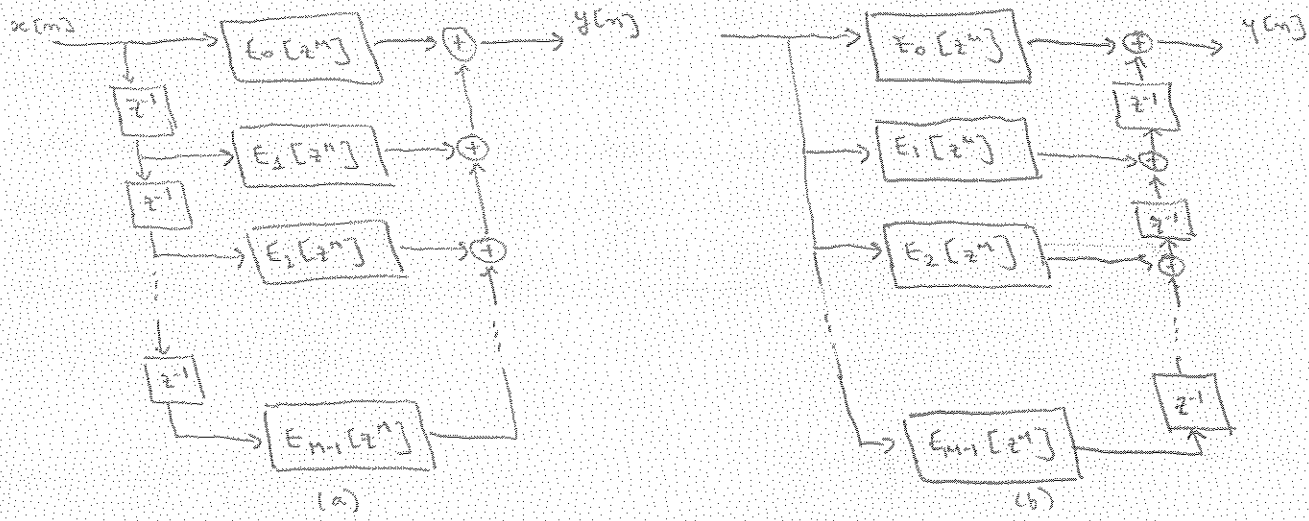


Fig. 13 Realization of an FIR filter based on a Type I polyphase decomposition. (a) direct and (b) transpose structures

An alternative representation of the transpose structure is obtained by using the notation

$$R_\ell[z^M] = E_{M-1-\ell}[z^M], \quad 0 \le \ell \le M-1$$

which results in the polyphase decomposition given by

$$H[z] = \sum_{\ell=0}^{M-1} z^{-(M-1-\ell)} R_\ell[z^M]$$

that is called Type II polyphase decomposition and is illustrated in Fig. 14 below

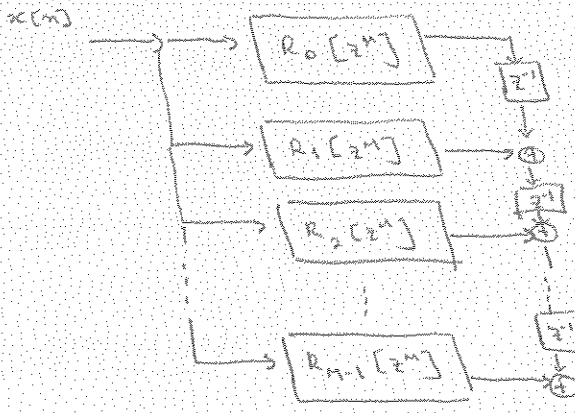


Fig. 14 Realization of an FIR filter based on a Type II polyphase decomposition

Computationally efficient decimator and interpolator structures employing linear-phase lowpass filters can be derived by applying a polyphase decomposition to the lowpass filters. Let us consider first the use of the polyphase decomposition in the realization of a decimation filter. This structure is depicted in Fig 15 below

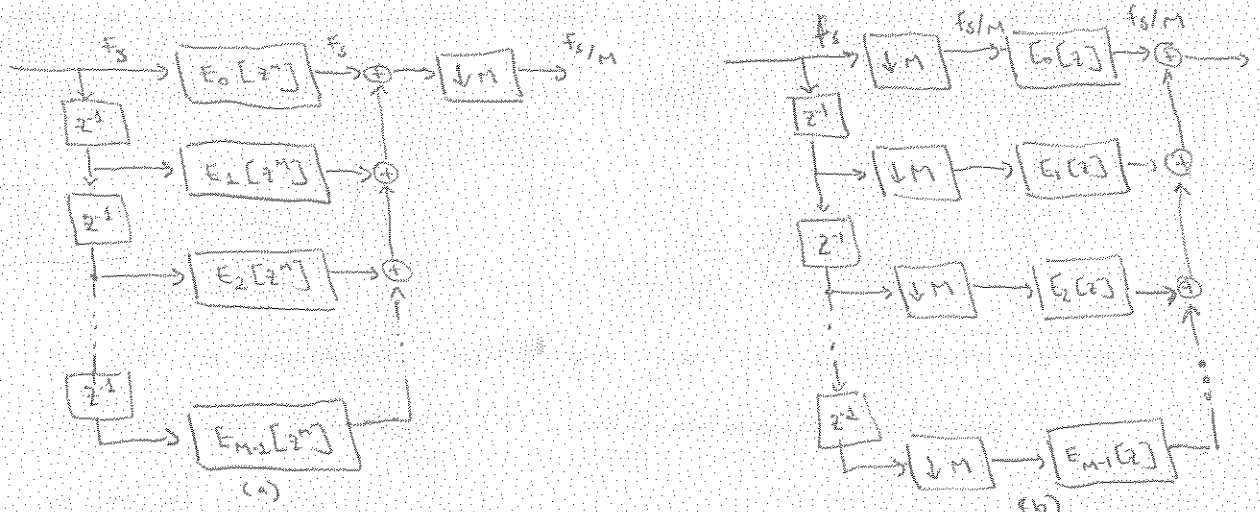


Fig. 15 Decimator implementation based on a polyphase decomposition

Since the decimator output is obtained by down-sampling the filter outputs by a factor of $M$, it is only necessary to compute operations at $n = \ldots, -2M, -M, 0, M, 2M, \ldots$ The computational requirements are $N$ multiplications and $(N-1)$ additions per sample. The structure of Fig 15 (b) is an alternative that stores less samples

Similar saving can be obtained for an interpolator structure as the one shown in Fig 16

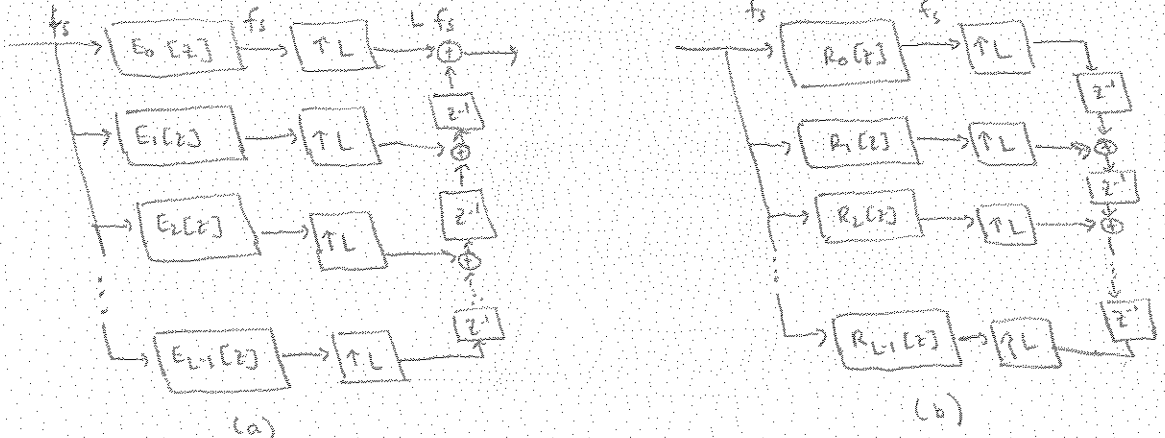


Fig. 16 Computationally efficient interpolator structures: (a) Type I polyphase decomposition and (b) Type II polyphase decomposition.

## D. Digital Filter Banks

There are applications where it is desirable to separate a signal into a set of subband signals occupying, usually nonoverlapping, portions of the original frequency band. Digital filter banks are an important tool to separate and combine signals in subbands.

A digital filter bank is a set of digital bandpass filters with either a common input or a summed output, as depicted in Fig. 17 below.

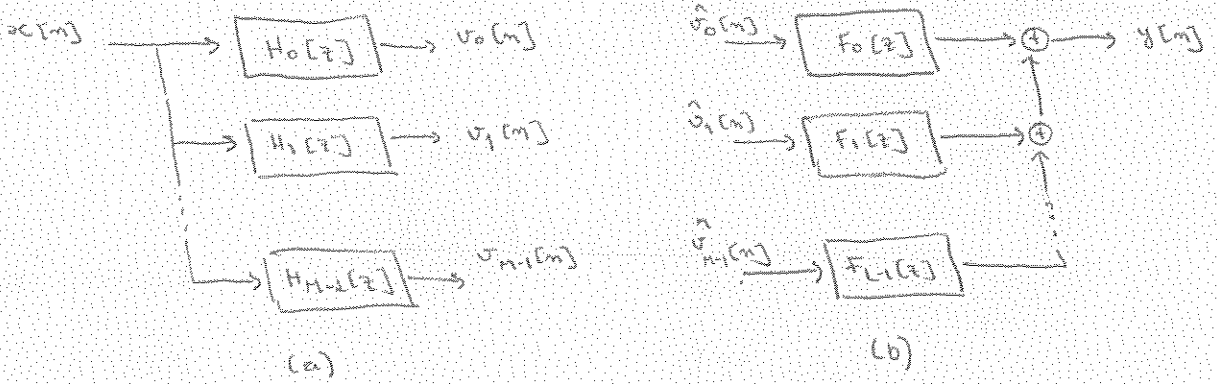


Fig. 17 (a) Analysis filter bank and (b) synthesis filter bank.

The structure in Fig. 17 (a) is called an M-band analysis filter bank with the subfilters $H_k[z]$ known as the analysis filters. It is used to decompose the input signal $x[n]$ into a set of M subband signals $v_k[n]$ with each subband signal occupying a portion of the original frequency band.

The dual of the analysis is the synthesis, whereby a set of subband signals $\hat{v}_k[n]$ is combined into one signal $y[n]$. The synthesis filter bank performs the task of gathering these signals with the help of the synthesis filters $f_k[z]$, as illustrated in Fig. 17 (b).

We now outline a simple technique for the design of a class of filter banks with equal passband widths. Let $H_0[z]$ represent a causal lowpass digital filter with an impulse response $h_0[n]$.

$$H_0[z] = \sum_{n=0}^{N} h_0[n] \cdot z^{-n},$$

which we assume to be an arbitrary filter.

Let us now assume that $H_0[z]$ has its passband edge $\omega_p$ and stopband edge $\omega_s$ around $\pi/M$, where $M$ is some arbitrary integer, as indicated in Fig. 18(a) below.

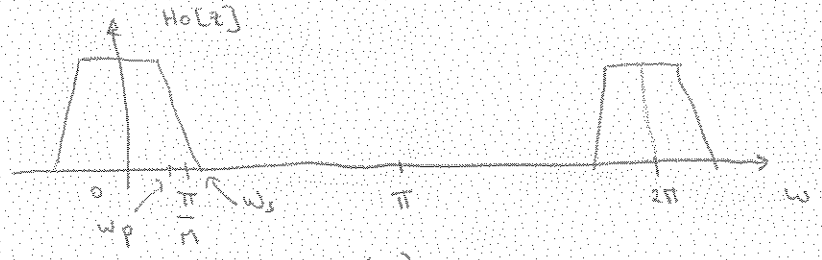


(a)

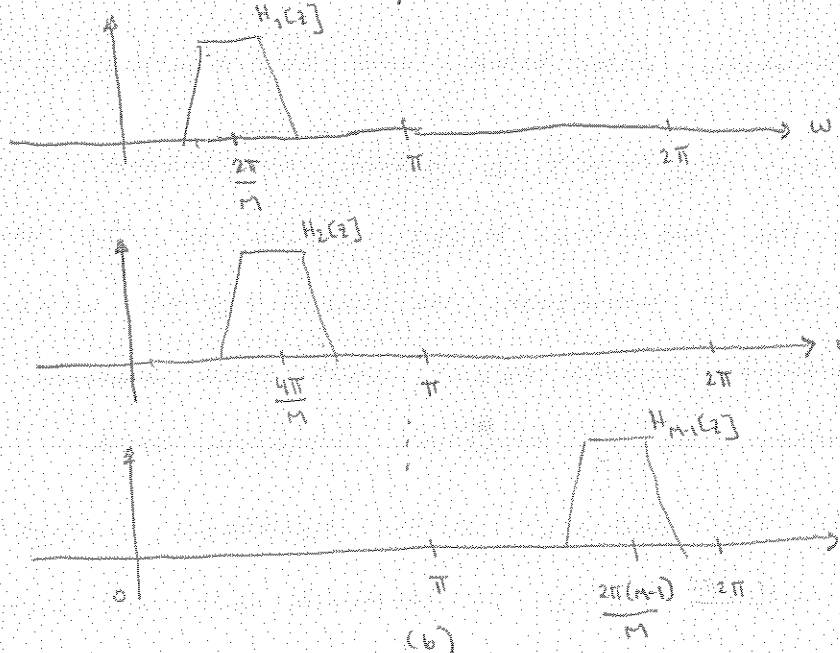


(b)

Fig. 18 The bank of $M$ filters $H_k[z]$ with uniformly shifted frequency responses.

Consider now the transfer function $H_k(z)$ whose impulse response is defined as

$$h_k[n] = h_0[n] \cdot W_M^{-kn}, \quad 0 \le k \le M-1,$$

where $W_M = e^{-j 2\pi/M}$. Thus, we have

$$H_k(z) = \sum_{n=0}^{\infty} h_k[n] \cdot z^{-n} = \sum_{n=0}^{\infty} h_0(n) \cdot \left(z W_M^k\right)^{-n}, \quad 0 \le k \le M-1,$$

$$= H_0[z W_M^k], \quad 0 \le k \le M-1.$$

with a corresponding frequency response

$$H_k(e^{j\omega}) = H_0\left(e^{j(\omega - 2\pi k/M)}\right), \quad 0 \le k \le M-1.$$

In other words, the frequency response of $H_k(z)$ is obtained by shifting the response of $H_0(z)$ to the right by an amount $\frac{2\pi k}{M}$. The responses of $H_1(z), H_2(z), \ldots, H_{M-1}(z)$ are shown in Fig 18 (b). Note that the corresponding impulse responses $h_k(n)$ are, in general, complex and hence $|H_k(e^{j\omega})|$ does not necessarily exhibit symmetry with respect to zero frequency. Fig. 18 (b) represents the responses of M-1 filters $H_1(z), H_2(z), \ldots, H_{M-1}(z)$ which are uniformly shifted versions of the response of the basic prototype filter $H_0(z)$ of Fig. 18 (a).

The M filters $H_k(z)$ could be used as the analysis filters in the analysis filter bank of Fig. 17(a) or as the synthesis filters $F_k(z)$ in the synthesis filter bank of Fig. 17 (b). Since the set of magnitude responses $|H_k(e^{j\omega})|$, $k = 0, 1, \ldots, M-1$ are uniformly shifted versions of a basic prototype $|H_0(e^{j\omega})|$, i.e., $|H_k(e^{j\omega})| = |H_0(e^{j(\omega - 2\pi k/M)})|$, the filter bank obtained is called a uniform filter bank.

# Polyphase Implementation of Uniform Filter Banks

Let Fig 11 (a) represent a uniform filter bank with the M analysis filters $H_k[z]$ related through

$$H_k[z] = H_0(z W_M^k), \quad 0 \le k \le M-1$$

The impulse responses $h_k(n)$ of the analysis filters are related according to

$$h_k[n] = h_0[n] \; W_M^{-kn}$$

Instead of realizing each analysis filter as a separate filter, it is possible to develop a computationally more efficient realization of the above described uniform filter bank.

Let the lowpass prototype transfer function $H_0(z)$ be represented in its M-band polyphase form as described by

$$H_0(z) = \sum_{l=0}^{M-1} z^{-l} \; E_l[z^M],$$

where $E_l[z]$ is the $l$th polyphase component of $H_0[z]$ given by

$$E_l[z] = \sum_{n=0}^{\infty} e_l[n] z^{-n} = \sum_{n=0}^{\infty} h_0[l+nM] z^{-n}, \quad 0 \le l \le M-1$$

Replacing $z$ with $z W_M^k$ in $H_0[z]$, we arrive at the M-band polyphase decomposition of $H_k[z]$.

$$H_k(z) = \sum_{l=0}^{M-1} z^{-l} W_M^{kl} \; E_l\left[z^M W_M^{kM}\right] = \sum_{l=0}^{M-1} z^{-l} W_M^{-kl} \; E_l(z^M), \quad 0 \le k \le M-1,$$

where we have used the identity $W_M^{kM} = 1$.

The above equation can be written as

$$H_k[z] = \begin{bmatrix} 1 & W_M^{-k} & W_M^{-2k} & \cdots & W_M^{-(M-1)k} \end{bmatrix} \begin{bmatrix} E_0[z^M] \\ z^{-1} E_1[z^M] \\ z^{-2} E_2[z^M] \\ \vdots \\ z^{-(M-1)} E_{M-1}[z^M] \end{bmatrix}, \quad k = 0, 1, \ldots M-1$$

These M equations can be combined into a matrix equation

$$\begin{bmatrix} H_0[z] \\ H_1[z] \\ H_2[z] \\ \vdots \\ H_{M-1}[z] \end{bmatrix} = M \cdot \underline{D}^{-1} \begin{bmatrix} E_0[z^M] \\ z^{-1} E_1[z^M] \\ z^{-2} E_2[z^M] \\ \vdots \\ z^{-(M-1)} E_{M-1}[z^M] \end{bmatrix},$$

where $\underline{D}$ denotes the DFT matrix

$$\underline{D} = \begin{bmatrix} 1 & 1 & 1 & \cdots & 1 \\ 1 & W_M^1 & W_M^2 & \cdots & W_M^{(M-1)} \\ 1 & W_M^2 & W_M^4 & \cdots & W_M^{2(M-1)} \\ \vdots & \vdots & \vdots & & \\ 1 & W_M^{(M-1)} & W_M^{2(M-1)} & & W_M^{(M-1)^2} \end{bmatrix}$$

An efficient implementation of the M-band analysis filter bank is shown in Fig. 19, where the prototype $H_0[z]$ is implemented in polyphase form. This is known as the uniform DFT analysis filter bank.

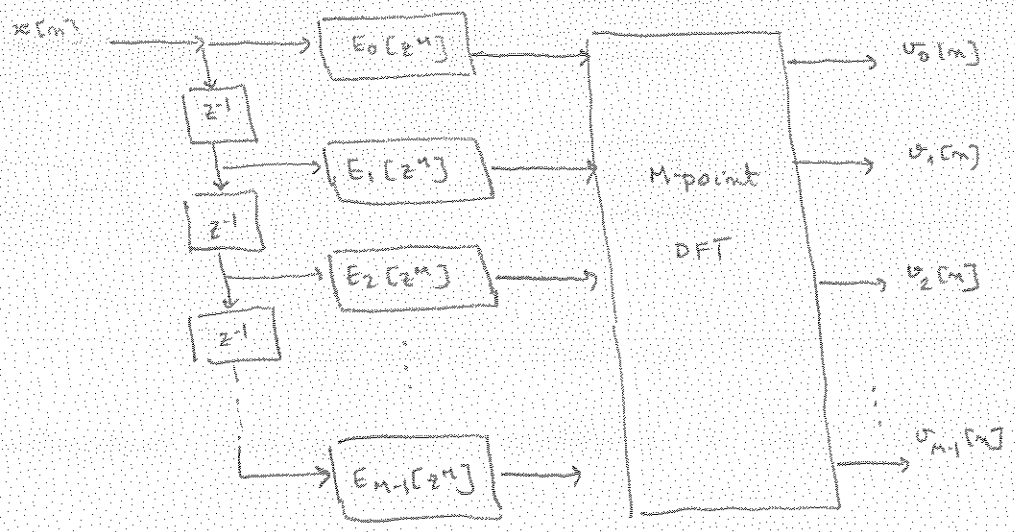


Fig. 19. Polyphase implementation of a uniform DFT analysis filter bank. where $H_k[z] = V_k[z] / X[z]$.

The computational complexity of the structure in Fig. 19 is much lower than that of Fig. 17 (a). For example, an M-band uniform DFT analysis filter bank based on an N-tap prototype FIR filter with the M-point DFT implemented using a radix-2 FFT algorithm requires a total of $(M/2)\log_2 M + N$ multipliers, whereas a direct implementation requires $N.M$ multiplications

Following a similar development to the analysis filter bank, we can derive the structure for a uniform DFT synthesis filter bank. Efficient realizations based on Types I and II polyphase decompositions of the prototype $H_0[z]$ are indicated in Fig. 20.

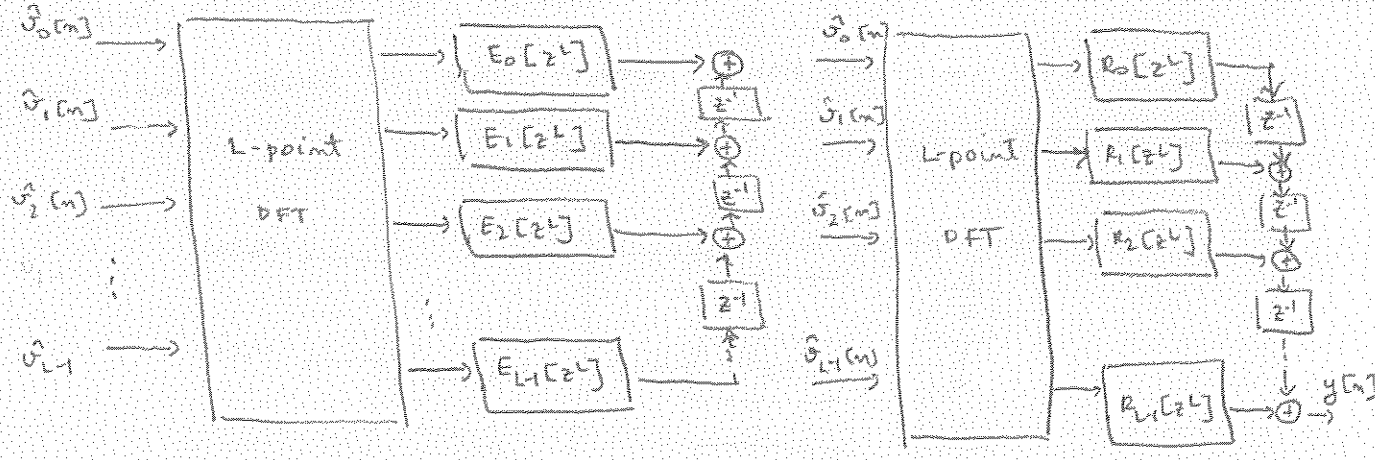


Fig. 20 Uniform DFT synthesis filter bank:

(a) Type I polyphase decomposition realization

(b) Type II polyphase decomposition realization.

Example 14.1 : Design of a Four-Channel Uniform DFT Filter Bank

We consider a fourth-band ($L=4$) linear-phase lowpass filter of length 23 using the windowed Fourier series approach.

$$E_0(z) = 0,0016 - 0,011\,z^{-1} + 0,063\,z^{-2} + 0,22\,z^{-3} - 0,027\,z^{-4} + 0,0038\,z^{-5}$$

$$E_1(z) = 0,0031 - 0,025\,z^{-1} + 0,14\,z^{-2} + 0,14\,z^{-3} - 0,025\,z^{-4} + 0,0031\,z^{-5}$$

$$E_2(z) = 0,0038 - 0,027\,z^{-1} + 0,22\,z^{-2} + 0,063\,z^{-3} - 0,011\,z^{-4} + 0,001\,z^{-5}$$

$$E_3(z) = 0,25\,z^{-2}$$

For $M=4$, we have

$$\begin{bmatrix} H_0(z) \\ H_1(z) \\ H_2(z) \\ H_3(z) \end{bmatrix} = \begin{bmatrix} 1 & 1 & 1 & 1 \\ 1 & j & -1 & -j \\ 1 & -1 & 1 & -1 \\ 1 & -j & -1 & j \end{bmatrix} \begin{bmatrix} E_0(z^4) \\ z^{-1}E_1(z^4) \\ z^{-2}E_2(z^4) \\ z^{-3}E_3(z^4) \end{bmatrix}$$

The four (4) analysis filters are given by

$$H_0(z) = E_0(z^4) + z^{-1}E_1(z^4) + z^{-2}E_2(z^4) + z^{-3}E_3(z^4)$$

$$H_1(z) = E_0(z^4) + j\,z^{-1}E_1(z^4) + (-z^{-2})E_2(z^4) + (-j)\,z^{-3}E_3(z^4)$$

$$H_2(z) = E_0(z^4) - z^{-1}E_1(z^4) + z^{-2}E_2(z^4) - z^{-3}E_3(z^4)$$

$$H_3(z) = E_0(z^4) - j\,z^{-1}E_1(z^4) - z^{-2}E_2(z^4) + j\,z^{-3}E_3(z^4).$$

A plot of the gain responses of the analysis filters of the four-channel uniform DFT filter bank is shown below in Fig. 2.1